

# Cyclic Biphalin Analogues Incorporating a Xylene Bridge: Synthesis, Characterization, and Biological Profile

Azzurra Stefanucci,<sup>†,⊥</sup> Alfonso Carotenuto,<sup>‡,⊥</sup> Giorgia Macedonio,<sup>†</sup> Ettore Novellino,<sup>‡</sup> Stefano Pieretti,<sup>§</sup> Francesca Marzoli,<sup>§</sup> Edina Szűcs,<sup>||</sup> Anna I. Erdei,<sup>||</sup> Ferenc Zádor,<sup>||</sup> Sándor Benyhe,<sup>||</sup> and Adriano Mollica<sup>\*,†,⊥</sup>

<sup>†</sup>Dipartimento di Farmacia, Università di Chieti-Pescara “G. d’Annunzio”, Via dei Vestini 31, 66100 Chieti, Italy

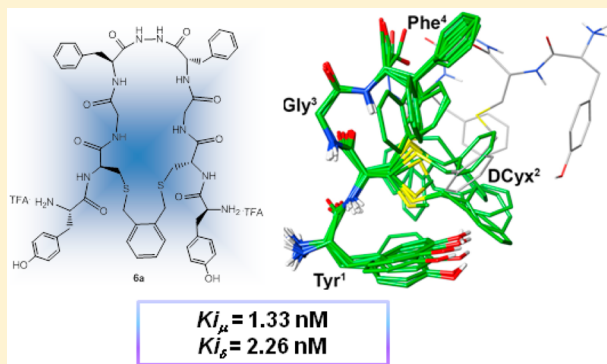
<sup>‡</sup>Dipartimento di Farmacia, Università di Napoli “Federico II”, Via D. Montesano, 49, 80131 Naples, Italy

<sup>§</sup>Istituto Superiore di Sanità, Centro Nazionale per la Ricerca e la Valutazione Preclinica dei Farmaci, Viale Regina Elena 299, 00161 Rome, Italy

<sup>||</sup>Institute of Biochemistry, Biological Research Center of the Hungarian Academy of Sciences, Temesvári krt. 62., H-6726 Szeged, Hungary

## Supporting Information

**ABSTRACT:** In this work we enhanced the ring lipophilicity of biphalin introducing a xylene moiety, thus obtaining three cyclic regioisomers. Novel compounds have similar *in vitro* activity as the parent compound, but one of these (6a) shows a remarkable increase of *in vivo* antinociceptive effect. Nociception tests have disclosed its significant high potency and the more prolonged effect in eliciting analgesia, higher than that of biphalin and of the disulfide-bridge-containing analogue (7).



**KEYWORDS:** Biphalin, CLIPS technology, xylene bridge, antinociception, opioids

Recently mixed  $\mu/\delta$  opioid ligands have shown significant potential as analgesics with novel biological profiles. Being the result of a “twin-drug approach” to the opioid peptides enkephalins, biphalin (Tyr<sup>1</sup>-D-Ala<sup>2</sup>-Gly<sup>3</sup>-Phe<sup>4</sup>-NH-NH-Phe<sup>4'</sup> ← Gly<sup>3'</sup> ← D-Ala<sup>2'</sup> ← Tyr<sup>1'</sup>) has an exceptional affinity for  $\mu$  and  $\delta$  receptors (MOR and DOR, respectively) with an EC<sub>50</sub> of about 1–4 nM; it has a highly potent antinociceptive effect (3-fold increase compared to morphine after i.c.v.), similar to that of etorphine.<sup>1</sup> Biphalin penetrates blood–brain barrier (BBB) well; hence, it can be systemically administered.<sup>2</sup> Furthermore, Yamazaki et al. reported biphalin’s potential to produce dependence upon chronic use.<sup>3</sup> A conclusive mechanism of action that could explain the unique *in vivo* potency has not been obtained, though it was speculated that it is related to its dual  $\mu/\delta$  bioactivity together with its capability to stimulate the formation of opioid receptor dimers.<sup>4</sup> The (MOR–DOR) dimers exhibit restricted distribution in the brain, and their abundance is increased in response to chronic morphine administration.<sup>5</sup> The  $\mu/\delta$  multitarget approach potentially represents a unique tool for the development of safe and potent therapeutics to treat chronic pain.<sup>6</sup> Numerous structure–activity relationships (SAR) studies have been reported on biphalin;<sup>1,7</sup> many of these focused on amino acid

substitution in positions 2,2' and 4,4',<sup>8,9</sup> supported also by molecular dynamics (MD) study.<sup>10</sup>

Constrained peptidomimetics obtained by global and/or local restrictions may also overcome some limitations typical of linear peptides (e.g., biphalin), such as low analgesic potency after s.c. administration and a moderate stability in human plasma.<sup>1</sup> In our previous works on cyclic biphalins, we found that D-Ala<sup>2-2'</sup> can be replaced by D-Cys and D-Pen residues followed by ring closure as a disulfide bridge to give analogues with increased *in vitro* affinity for  $\mu/\delta$ -opioid receptors and *in vivo* antinociceptive effect.<sup>11,12</sup>

In this letter, we further modified the biphalin structure with the incorporation of a xylene bridge by the chemical linkage of peptides onto scaffolds (CLIPS) technology,<sup>13</sup> recently applied by our group for the preparation of cyclic DPDPE analogues.<sup>14</sup> This modification was aimed at improving the pharmacological parameters as well as the BBB permeability and plasma stability of the new compounds with respect to biphalin. We synthesized and fully characterized three novel biphalin analogues in which

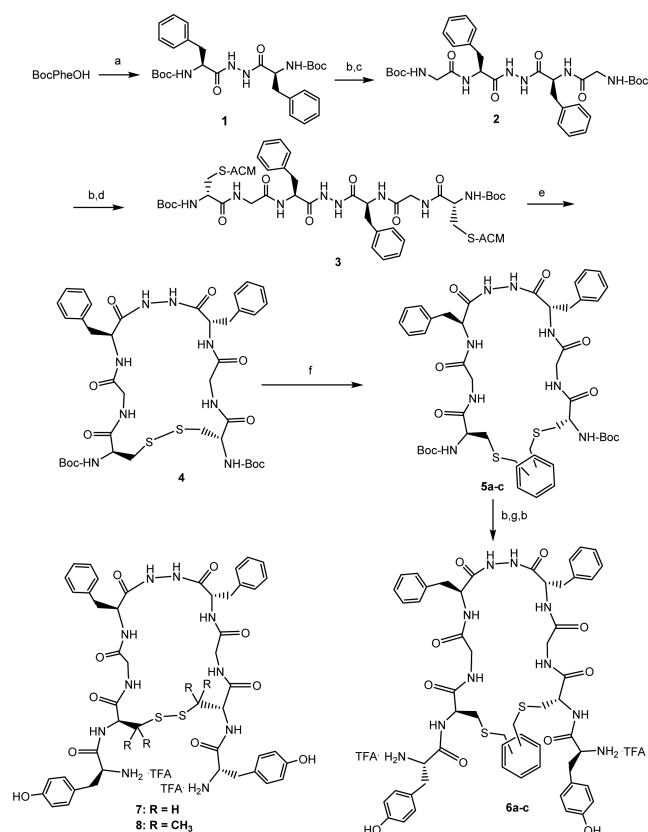
Received: May 18, 2017

Accepted: July 12, 2017

Published: July 12, 2017

the two thiol groups of the D-Cys residues in position 2,2' have been linked through using different dibromoxylene regioisomers (*o*-dibromoxylene, *m*-dibromoxylene, and *p*-dibromoxylene for **6a–c**, respectively). These compounds have been tested *in vitro* for  $\mu/\delta$  receptor binding assays and G-protein activation and, finally, for *in vivo* antinociception tests, to evaluate the analgesic potency compared to that of biphalin and its disulfide bridge containing cyclic analogue **7**, previously published by our group.<sup>11</sup> The new analogues were prepared via solution phase peptide strategy (Scheme 1).<sup>12,15</sup> The

### Scheme 1. Synthesis of Novel Cyclic Analogues **6a–c**<sup>a</sup>



<sup>a</sup>Reagents and conditions: (a) hydrazine monohydrate, EDC·HCl, HOBT anhydrous, NMM, DMF, 0 °C for 20 min, then r.t. 24 h, 95% yield. (b) TFA/DCM 1:1, r.t. 3 h, quantitative. (c) Boc-Gly-OH, EDC·HCl, HOBT anhydrous, NMM, DMF, 0 °C, 20 min, then r.t. 24 h, 96% yield. (d) Boc-D-Cys(ACM)-OH, EDC·HCl, HOBT anhydrous, NMM, DMF, 0 °C, 20 min, then r.t. 24 h, 90% yield. (e) I<sub>2</sub>, MeOH, 3 h at r.t. then ascorbic acid, quantitative. (f) TCEP, DMF for 1 h at r.t., then dibromoxylene regioisomers at r.t., overnight; **5a**, 97% yield; **5b**, 92% yield; **5c**, 88% yield after RP-HPLC purification. (g) Boc-Tyr-OH, EDC·HCl, HOBT anhydrous, NMM, DMF, 0 °C for 20 min, then r.t. 24 h.

incorporation of xylene bridge was achieved through the cyclic intermediate *c*[D-Cys-Gly-Phe-NH]<sub>2</sub> (**4**) via one-pot reduction/side chain-to-side chain type cyclization reaction, using a modified procedure reported by Smith et al.;<sup>16</sup> due to the small size and moderate polarity of our cyclic peptides, aqueous buffers are not required,<sup>12,17</sup> and thus, DMF was used (for further details, see Experimental Procedures). The crude cyclic intermediates **5a–c** were used in the final coupling reaction, without any further modifications, to give products **6a–c** as TFA salts in excellent yields. Cyclic biphalin analogue **7** was

also prepared as previously described by Mollica et al.<sup>12</sup> The final cyclic peptides were purified by RP-HPLC and characterized by NMR, LRMS, and UPLC–MS (Figures S1–S6, Supporting Information).

Novel compounds **6a–c** were tested for their affinity toward opioid receptors  $\mu$  and  $\delta$ , which were the only targets of biphalin and all its derivatives developed until now. Compounds **7** and **8** were also reported for comparison. Compared to biphalin, cyclic analogues **6a–c** and **7–8** had a slightly lower affinity on MOR; however, their  $K_i$  values still remained in the nanomolar range (Table 1 and Figure S7,

**Table 1. MOR and DOR Affinity of **6a–c**; Biphalin and **7** Were Also Tested for Comparison<sup>a</sup>**

comps	$K_i$ (nM)		selectivity ratio DOR/MOR
	[ <sup>3</sup> H]DAMGO (MOR)	[ <sup>3</sup> H]IleDelt II (DOR)	
biphalin	0.79	3.5	4.4
<b>6a</b>	1.33	2.26	1.8
<b>6b</b>	1.73	3.81	2.2
<b>6c</b>	1.61	2.52	1.5
<b>7</b>	6.06	5.25	0.9
<b>8</b> <sup>b</sup>	1.90	5.20	2.7

<sup>a</sup>The affinity values are represented by  $K_i$ , which was calculated based on [<sup>3</sup>H]DAMGO and [<sup>3</sup>H]IleDelt II competition binding curves (see Figure S7) as described in the Data Analysis section. Selectivity ratios were calculated according to  $K_i$  values. <sup>b</sup>Reported in ref 12.

Supporting Information). In case of DOR, the results were less consistent: **6a** and **6c** showed a slightly higher affinity than biphalin. From the binding data, it can be argued that analogues **6a–c** have a reduced MOR selectivity compared to biphalin (Table 1). Compound **7** showed a similar affinity to MOR; thus, the DOR/MOR selectivity ratio remained close to unity (Table 1). Finally, compound **8** had similar MOR affinity and a slightly reduced DOR affinity compared to **6a–c**. Transmembrane signaling of the biphalin analogues via heterotrimeric G-proteins was studied in [<sup>35</sup>S]GTP $\gamma$ S binding experiments in rat brain membranes. The parent compound biphalin displayed the highest stimulation (efficacy) thus being designated as full agonist, while the derivatives exhibited partial agonist properties characterized by lower efficacy levels in this assay (Table 2 and Figure S8, Supporting Information).

**Table 2. Maximal G-Protein Efficacy ( $E_{max} \pm SEM$ ) and Ligand Potency  $EC_{50}$  of **6a–c**, **7**, and Biphalin<sup>a</sup>**

compd	$E_{max} \pm SEM$ (%)	$EC_{50}$ (nM)
biphalin	176.9 $\pm$ 4.9	75.4
<b>6a</b>	137.4 $\pm$ 5.6	247.2
<b>6b</b>	160.2 $\pm$ 7.0	212.6
<b>6c</b>	149.9 $\pm$ 6.6	87.4
<b>7</b>	145.9 $\pm$ 3.6	508.3

<sup>a</sup>The values were calculated according to dose-response binding curves in Figure S8 performed in [<sup>35</sup>S]GTP $\gamma$ S binding assays as described in the Data Analysis section.

In case of **6a** and **6c**, the reduction in the  $E_{max}$  value was more prominent compared to **6b**, while the potency of **6c** was very close to the potency value of biphalin (Table 2). Compound **7** displayed a similar  $E_{max}$  value as that of **6c**, but the potency of the last was the lowest among the cyclic compounds (Table 2).

Compound **6b** showed similar efficacy but significantly lower potency than biphalin, while **6c** showed similar potency but lower efficacy than biphalin (Table 2). From the G-protein activation assay, we can assume that compounds **6a–c** are partial  $\mu/\delta$ -opioid agonists and more potent than compound **7**. Encouraged by the *in vitro* preliminary results, cyclic analogues **6a–c** were tested *in vivo* in two pain models (Figure 1). Product **6a** performed better than the other compounds to elicit antinociception in *in vivo* tests, being able to induce long

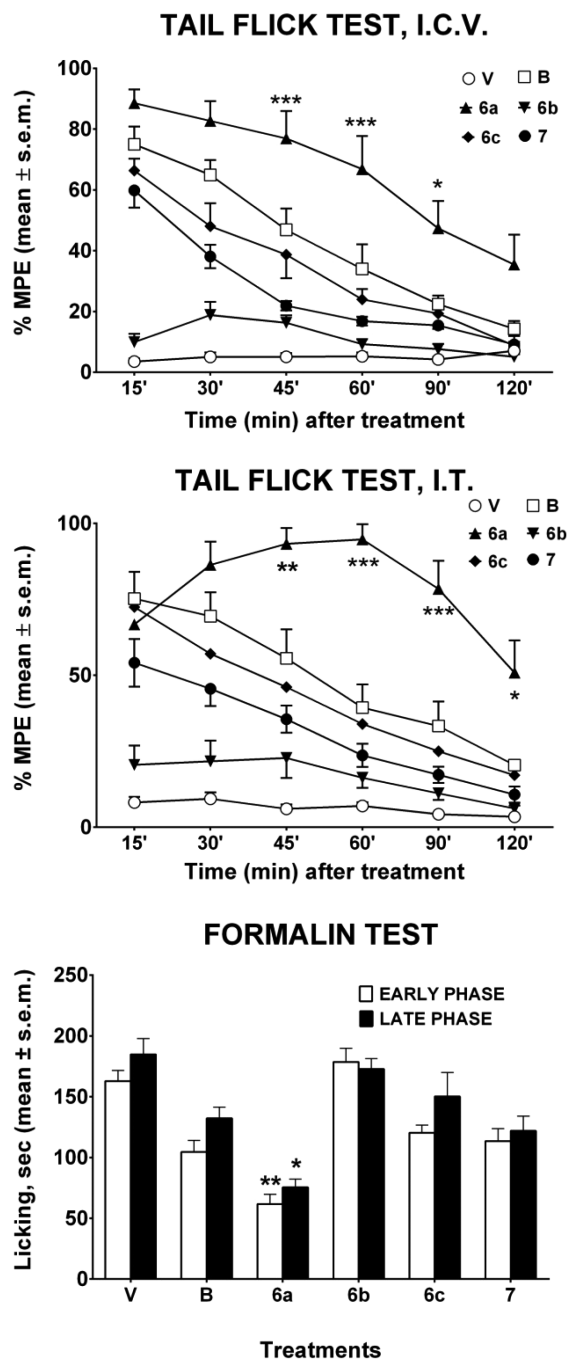


**Figure 1.** Tail flick and formalin tests for cyclic analogues **6a–c**. In the tail flick test, compounds were administered i.c.v. or i.t. at the dose of 0.01 nmol/animal. In the formalin test, compounds were administered s.c. at the dose of 0.1 nmol/animal. V is for vehicle-treated animals; B is for biphalin-treated animals; %MPE is for maximal percent effect. \*\*\* $P < 0.001$ , \*\* $P < 0.01$ , and \* $P < 0.05$  vs B.  $N = 10–12$ .

lasting antinociception effect from 45' to 90' after i.c.v. administration and from 45' to 120' after i.t. administrations in the tail flick (TF) test. Formalin test confirmed that compound **6a** had the highest analgesic effect compared to the other compounds, including biphalin. Compound **6a** was able to reduce formalin induced pain behavior both in the early and in the late phase of the test after s.c. administration. The last observation suggests an improved crossing of the BBB of **6a** compared to biphalin as assumed in the design strategy. Product **6b** induced slight antinociceptive effect, and product **6c** showed similar effects to those observed after biphalin administration both in the tail flick and formalin test. Interestingly the insertion of different xylene regioisomers deeply influenced the *in vivo* results, as reported also for DPDPE cyclic analogues.<sup>14</sup> Among the new cyclic biphalin analogues tested, only **6a** incorporating the *o*-xylene regioisomer resulted to be more potent than the parent compound after i.c.v, i.t., and s.c. administrations.

The enzymatic stability of biphalin and its cyclic analogue **6a** was evaluated by incubation at 37 °C in human plasma. Degradation curves (Figure S9, Supporting Information) were plotted as the total amount of remaining parent compound (expressed as  $\mu\text{g/mL}$ ) versus time (as minutes), revealing improved stability of **6a** compared to biphalin in human plasma.<sup>15</sup> The degradation half-life ( $t_{1/2}$ ) of biphalin and **6a** in human plasma was obtained by least-squares linear regression analysis of peptide peak area versus time (see Supporting Information). Results indicate that biphalin showed a half life of  $33 \pm 2$  min in the plasma, whereas **6a** exhibited significantly longer half life compared to biphalin since the plasma  $t_{1/2}$  of cyclic analogue was  $87 \pm 7$  min.

Compounds **6a**, **6b**, and **6c** displayed nanomolar activities in the receptor binding assays. Interestingly, in [<sup>35</sup>S]GTP $\gamma$ S binding experiments, **6a** possessed rather partial agonist property, while the efficacy of **6b** remained close to that found with the reference compound biphalin. However, in the *in vivo* tests, **6b** seemed to be carrying only weak effects, despite its good *in vitro* affinity. Since the only difference among **6a–c** compounds is in the structure of the xylene bridge (ortho-, meta-, and para-, respectively), we have to suggest that these minor changes might be among the reasons. However, very similar binding profiles of **6a–c** to MOR and DOR receptors reasonably rule out the possibility of different 3D structures for the three peptides. The good *in vitro* versus bad *in vivo* effects can be explained due to different bioavailabilities or altered BBB passage of the analogues; both need to be investigated further.

A conformational analysis of the analogue **6a** was carried out by solution NMR. Dodecylphosphocholine (DPC) micelle solution was used to mimic a membrane environment considering that opioid peptides interact with membrane receptors.<sup>18</sup> Complete <sup>1</sup>H NMR assignment was accomplished using the standard Wüthrich protocol (Supporting Information, Table S1).<sup>19</sup> Due to the symmetric nature of the compound, only one set of signals was observed for the two symmetric sides of the molecule. A few diagnostic cross-peaks could be observed in the NOESY spectrum of **6a**; two  $d_{\alpha\text{N}}(i, i + 2)$  correlations between residues 1–3 and 2–4 and a  $d_{\text{NN}}(i, i + 2)$  between residues 2–4 are typical of folded structures. Furthermore, NOE cross peaks between the aromatic proton signals of both Tyr<sup>1</sup> and Phe<sup>4</sup> with the signals of the xylene-derived portion indicate that aromatic moieties are spatially close. Using the NMR data as input (Table S2, Supporting Information), structure calculations by restrained simulated

annealing was performed. NOEs were considered to involve residues from the same monomer. In fact, unrestrained MD simulations on peptide **6a** demonstrated that, during the simulations, the two monomers were too far, on average, to observe intermonomer dipolar couplings. Figure S10 (Supporting Information) illustrates this point considering the diagnostic distance between H $\alpha$  of residue 2 and HN of residue 4 or residue 4' during the MD. As observed, only the intramonomer distance was compatible with the observed NOE ( $d_{\alpha N} \approx 5 \text{ \AA}$ ). Restrained calculations gave the structure shown in Figure 2a. Compound **6a** shows a well-defined structure

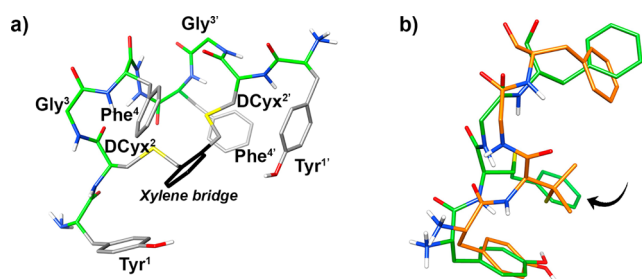


**Figure 2.** (a) Lowest energy conformer of peptide **6a**. Heavy atoms have different colors (nitrogen, blue; oxygen, red; sulfur, yellow; backbone carbon, green; side chain carbon, gray; aromatic linker, dark gray). Most of the hydrogen atoms are hidden for a better view. Residue indicated as D-Cyx was the residue incorporating the aryl linker. (b) Superposition of the lowest energy conformer of peptides **6a** (residues 1–4, carbon atoms in green) and **8** (orange). Position of aryl linker is evidenced by an arrow.

encompassing residues 1–4 or 1'–4' (backbone rmsd values are 0.19 and 0.24  $\text{\AA}$ , respectively, for the 10 lowest energy calculated structures; Supporting Information Figure S11).

An inverse  $\gamma$ -turn (distorted, Table S3, Supporting Information) centered on Gly<sup>3</sup> is seen in the structure ensemble. Tyr<sup>1</sup> side chain is in *trans*-orientation, while Phe<sup>4</sup> side chain is both *trans* and *g*<sup>-</sup> oriented (about 50% of the calculated structures each). As expected from the NOE cross-peaks between the aromatic rings,  $\pi$ -stackings involving Tyr<sup>1</sup> and/or Phe<sup>4</sup> with a xylene aromatic ring were observed in most of the obtained conformers. Interestingly, the spatial distribution of the peptide side chains is similar to that recently reported for its D-Pen containing analogue **8** (Figure 2b).<sup>12</sup> In fact, compound **8** displayed a singular conformation with a sandwich-like  $\pi$ -CH<sub>3</sub>- $\pi$  geometry involving the three side chains of the peptide. The observation of such structural similarity between the two cyclic active analogues of biphalin, i.e., **6a** and **8**, is in accordance with their similar MOR and DOR binding profiles (Table 1), and this prompted us to investigate whether also the linear parent peptide, biphalin, retains this peculiarity.

Using the same steps in the conformational analysis, the structure depicted in Figure 3a was obtained as the most stable conformer of biphalin in DPC micelle solution. Biphalin structure proved to be more flexible as expected considering its linear nature (backbone rmsd 0.42  $\text{\AA}$  for the 10 lowest energy calculated structures; Supporting Information Figure S12), but it still shares a similar side chain topology with **6a** and **8**, as evidenced in Figure 3b. Again, the aromatic rings of Tyr<sup>1</sup> and Phe<sup>4</sup> tend to be close to the methyl group of D-Ala<sup>2</sup> in accordance with the NOE-derived constraints connecting protons belonging to those groups (Table S2). Distances

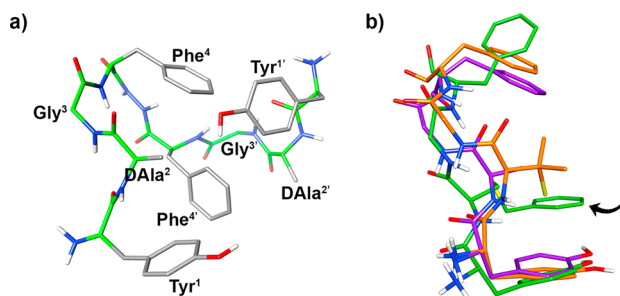


**Figure 3.** (a) Lowest energy conformer of biphalin. Heavy atoms have different colors (nitrogen, blue; oxygen, red; sulfur, yellow; backbone carbon, green; side chain carbon, gray). Most of the hydrogen atoms are hidden for a better view. (b) Superposition of the lowest energy conformer of biphalin (residues 1–4, carbon atoms in violet) with peptides **6a** (green) and **8** (orange). Aryl linker is evidenced by an arrow.

among pharmacophoric points in the calculated structures are in accordance with their activity profiles. In fact, in calculated structures of both **6a** and biphalin, the distance between the aromatic rings of Tyr<sup>1</sup> and Phe<sup>4</sup> was about 12.5  $\text{\AA}$  in conformers showing the *trans*-rotamers of Phe<sup>4</sup> and about 7.5  $\text{\AA}$  when Phe<sup>4</sup> was in *g*-orientation, thus fitting both the MOR (10–13  $\text{\AA}$ )<sup>20</sup> and DOR (about 7  $\text{\AA}$ )<sup>21</sup> pharmacophores.

The goal of this work was to design a series of novel cyclic biphalins able to bind at the  $\mu$ - and  $\delta$ -opioid receptors with reasonable affinity to produce antinociception and a longer lasting analgesia than the parent linear and disulfide bridge containing biphalin analogues. Three novel compounds have been synthesized by using the first generation CLIPS approach to constrain and cyclize side chains of D-Cys<sup>2,2'</sup> residues. Overall, the structural modifications in biphalin resulted in a slightly reduced *in vitro* affinity for MOR (Tables 1 and 2). Interestingly, novel compound **6a** is significantly more potent than biphalin and parent compound **7** and elicits antinociception in all *in vivo* assays (Figure 1). In particular, a long lasting antinociceptive effect after s.c. injection could be the result of improved plasma stability (Figure S9) and could indicate a better BBB penetration of **6a** compared to biphalin. Conformational analysis revealed that side chain orientation of **6a** is similar to that observed in both linear and cyclic active analogues (Figures 2 and 3). Reduced structural flexibility of **6a** compared to biphalin can tentatively explain some differences in terms of receptor affinity and efficacy observed between them. Compound **6a** yielded very promising results in view of future development of cyclic peptides for pain treatment.

## EXPERIMENTAL PROCEDURES

**Chemistry.** All reagents, solvents, and human plasma have been purchased by Sigma-Aldrich (MI, Italy). Synthesis of the cyclic analogues **6a–c** was performed in solution phase using the *N*<sup>ε</sup>-Boc strategy, starting from the coupling reaction between hydrazine and Boc-Phe-OH, with repeated steps of coupling/purification/deprotection of the intermediate products, following the procedures reported by Mollica et al. (Scheme 1).<sup>11,15</sup> Deprotection of *N*<sup>ε</sup>-tert-butylloxycarbonyl group was performed using TFA/CH<sub>2</sub>Cl<sub>2</sub> 1:1 for 1 h, under nitrogen atmosphere. The intermediate TFA salts were used for subsequent reactions without further purification. Boc-protected intermediate products were purified by silica gel column chromatography or, in the case of scarcely soluble products, by trituration in EtOAc. The reduction/side chain-to-side chain type cyclization reaction was performed as follows. Intermediate **4** (110 mg, 1 equiv) was dissolved in DMF (400 mL) at r.t. under N<sub>2</sub> atmosphere.

TCEP (0.28 mL, 1.1 equiv) was added, and the reaction mixture was stirred at r.t. for 1 h. Then the dibromoxylene isomer was added stirring overnight. The solvent was removed by rotary evaporator, and the residue was washed with deionized water and dried in vacuum, affording a crude solid product to use as such in the following coupling reaction with Boc-Tyr-OH.

Final products **6a–c** were purified by RP-HPLC using a Waters XBridge Prep BEH130 C18, 5.0  $\mu\text{m}$ , 250 mm  $\times$  10 mm column at a flow rate of 4 mL/min on a Waters Binary pump 600, using as eluent a linear gradient of H<sub>2</sub>O/acetonitrile–0.1% TFA ranging from 5% acetonitrile to 90% acetonitrile in 32 min. The identity of the *N*<sup>tr</sup>-Boc-protected products was confirmed by NMR analysis on a Varian VXR 300 MHz and mass spectrometry ESI–LRMS. The purity of all final TFA salts was confirmed by NMR analysis, ESI–LRMS, and analytical RP-HPLC recorded at 236 and 268 nm (C18-bonded 4.6 mm  $\times$  150 mm) at a flow rate of 1 mL/min, using as eluent a gradient of H<sub>2</sub>O/acetonitrile–0.1% TFA ranging from 5% acetonitrile to 95% acetonitrile in 32 min, and was found to be  $\geq 95\%$  (see [Supporting Information](#)). MS–UPLC data and HPLC chromatograms of the final products are reported in the [Supporting Information](#) (Figures S1–S6).

**2TFA-c(Tyr-D-Cys-Gly-Phe-NH)<sub>2</sub> o-Xylene (6a).** 80% overall yield; *R*<sub>t</sub> (HPLC) = 18.78 min. <sup>1</sup>HNMR (DMSO-*d*<sub>6</sub>)  $\delta$ : 2.34–2.65 (4H, m, Tyr  $\beta$ CH<sub>2</sub>; 4H, m, Phe  $\beta$ CH<sub>2</sub>), 2.71 (4H, s, CH<sub>2</sub> xylene), 2.91 (4H, d, D-Cys  $\beta$ CH<sub>2</sub>), 3.03 (4H, m, Gly  $\alpha$ CH<sub>2</sub>), 3.91–4.11 (2H, t, Tyr  $\alpha$ CH; 2H, t, Phe  $\alpha$ CH), 4.71–4.81 (2H, m, D-Cys  $\alpha$ CH), 6.61 (4H, dd, Tyr Ar), 7.01 (4H, dd, Tyr Ar), 7.09–7.19 (10H, m, Phe Ar and 4H xylene Ar), 8.04–8.21 (6H, d, Tyr NH<sub>3</sub><sup>+</sup> and 2H, d, D-Cys), 8.68–8.82 (2H, d, Phe NH and 2H, t, Gly NH), 9.33 (2H, s, OH), 10.36 (2H, s, NH-NH). ESI–LRMS calcd for C<sub>54</sub>H<sub>62</sub>N<sub>10</sub>O<sub>10</sub>S<sub>2</sub> *m/z*: 1074.4; found 1075.8 [M + H]<sup>+</sup>.

**2TFA-c(Tyr-D-Cys-Gly-Phe-NH)<sub>2</sub> m-Xylene (6b).** 75% overall yield; *R*<sub>t</sub> (HPLC) = 18.14 min. <sup>1</sup>HNMR (DMSO-*d*<sub>6</sub>)  $\delta$ : 2.41–2.25 (4H, m, Tyr  $\beta$ CH<sub>2</sub>; 4H, m, Phe  $\beta$ CH<sub>2</sub>), 2.54 (4H, s, CH<sub>2</sub> xylene), 2.77 (4H, d, D-Cys  $\beta$ CH<sub>2</sub>), 2.95 (4H, m, Gly  $\alpha$ CH<sub>2</sub>), 3.70–4.81 (2H, t, Tyr  $\alpha$ CH; 2H, t, Phe  $\alpha$ CH), 4.67–4.72 (2H, m, D-Cys  $\alpha$ CH), 6.66 (4H, dd, Tyr Ar), 7.05 (4H, dd, Tyr Ar), 7.18–7.31 (10H, m, Phe Ar and 4H xylene Ar), 8.01 (6H, d, Tyr NH<sub>3</sub><sup>+</sup>), 8.18 (2H, d, D-Cys), 8.68 (2H, t, Gly NH), 8.79 (2H, d, Phe NH), 9.34 (2H, s, OH), 10.39 (2H, s, NH-NH). ESI–LRMS calcd for C<sub>54</sub>H<sub>62</sub>N<sub>10</sub>O<sub>10</sub>S<sub>2</sub> *m/z*: 1074.4; found 1075.6 [M + H]<sup>+</sup>.

**2TFA-c(Tyr-D-Cys-Gly-Phe-NH)<sub>2</sub> p-Xylene (6c).** 79% overall yield; *R*<sub>t</sub> (HPLC) = 23.10 min. <sup>1</sup>HNMR (DMSO-*d*<sub>6</sub>)  $\delta$ : 2.46–2.55 (4H, m, Tyr  $\beta$ CH<sub>2</sub>; 4H, m, Phe  $\beta$ CH<sub>2</sub>), 2.82 (4H, s, CH<sub>2</sub> xylene), 3.01 (4H, d, D-Cys  $\beta$ CH<sub>2</sub>), 3.37 (4H, m, Gly  $\alpha$ CH<sub>2</sub>), 3.65–4.07 (2H, t, Tyr  $\alpha$ CH; 2H, t, Phe  $\alpha$ CH), 4.68 (2H, m, D-Cys  $\alpha$ CH), 6.71 (4H, dd, Tyr Ar), 7.05 (4H, dd, Tyr Ar), 7.18–7.24 (10H, m, Phe Ar and 4H xylene Ar), 8.01 (6H, d, Tyr NH<sub>3</sub><sup>+</sup>), 8.21 (2H, d, D-Cys), 8.61 (2H, t, Gly NH), 8.79 (2H, d, Phe NH), 9.36 (2H, s, OH), 10.42 (2H, s, NH-NH). ESI–LRMS calcd for C<sub>54</sub>H<sub>62</sub>N<sub>10</sub>O<sub>10</sub>S<sub>2</sub> *m/z*: 1074.4; found 1075.6 [M + H]<sup>+</sup>.

## ■ ASSOCIATED CONTENT

### Supporting Information

The Supporting Information is available free of charge on the ACS Publications website at DOI: [10.1021/acsmedchemlett.7b00210](https://doi.org/10.1021/acsmedchemlett.7b00210).

Details of compound characterization, biological assays, plasma stability, and NMR structural analysis ([PDF](#))

## ■ AUTHOR INFORMATION

### Corresponding Author

\*E-mail: [a.mollica@unich.it](mailto:a.mollica@unich.it).

### ORCID

Adriano Mollica: 0000-0002-7242-4860

## Author Contributions

<sup>†</sup>These authors contributed equally. The manuscript was written through contributions of all authors. All authors have given approval to the final version of the manuscript.

## Funding

Part of this study was supported by a NKFI basic research grant 108,518 provided by the National Research Development and Innovation Office, Budapest, Hungary.

## Notes

The authors declare no competing financial interest.

## ■ ABBREVIATIONS

DOR,  $\delta$ -opioid receptor; CLIPS, chemical linkage of peptides onto scaffolds; EDC, 1-ethyl-(3-(dimethylamino)propyl)-carbodiimide; ACM, acetamidomethyl; [3H]-DAMGO, [3H]-[D-Ala(2), N-Me-Phe-(4), Gly-ol(5)] enkephalin; [3H]Ile-DeltII, [3H]Ile(5,6)-deltorphinII; DPDPE, D-Pen<sup>2</sup>,D-Pen<sup>5</sup>-enkephalin; HOBt, 1-hydroxybenzotriazole; i.c.v., intracerebroventricular; MOR,  $\mu$ -opioid receptor; D-Pen, D-penicillamine; s.c., subcutaneous; NMM, N-methylmorpholine; TCEP, tris(2-carboxyethyl)phosphine; EtOAc, ethyl acetate; RP-HPLC, reversed phase high performance liquid chromatography; TF, tail flick test; DPC, dodecylphosphocholine

## ■ REFERENCES

- (1) Cowell, S. C.; Lee, Y. S. Biphalin: the foundation of bivalent ligand. *Curr. Med. Chem.* **2016**, *23*, 3267–3284.
- (2) Kosson, A.; Krizbai, I.; Leśniak, A.; Beręsewicz, M.; Sacharczuk, M.; Kosson, P.; Nagyoszi, P.; Wilhelm, I.; Kleczkowska, P.; Lipkowski, A. W. Role of the blood-brain barrier in differential response to opioid peptides and morphine in mouse lines divergently bred for high and low swim stress-induced analgesia. *Acta Neurobiol. Exp.* **2014**, *74*, 26–32.
- (3) Yamazaki, M.; Suzuki, T.; Narita, M.; Lipkowski, A. W. The opioid peptide biphalin induces less physical dependence than morphine. *Life Sci.* **2001**, *69*, 1023–1028.
- (4) Law, P. Y.; Erickson-Herbrandson, L. J.; Zha, Q. Q.; Solberg, J.; Chu, J.; Sarre, A.; Loh, H. H. Heterodimerization of  $\mu$ - and  $\delta$ -opioid receptors occurs at the cell surface only and requires receptor-G protein interactions. *J. Biol. Chem.* **2005**, *280*, 11152–11164.
- (5) Cahill, C. M.; Morinville, A.; Lee, M. C.; Vincent, J. P.; Collier, B.; Beaudet, A. Prolonged morphine treatment targets opioid receptors to neuronal plasma membranes and enhances-mediated antinociception. *J. Neurosci.* **2001**, *21*, 7598–7607.
- (6) Fujita, W.; Gomes, I.; Devi, L. A. Revolution in GPCR signalling: opioid receptor heteromers as novel therapeutic targets: IUPHAR Review 10. *Br. J. Pharmacol.* **2014**, *171*, 4155–4176.
- (7) Bonney, I. M.; Foran, S. E.; Marchand, J. E.; Lipkowski, A. W.; Carr, D. B. Spinal antinociceptive effects of AAS01, a novel chimeric peptide with opioid receptor agonist and tachykinin receptor antagonist moieties. *Eur. J. Pharmacol.* **2004**, *488*, 91–99.
- (8) Fraczak, O.; Lasota, A.; Lesniak, A.; Lipkowski, A. W.; Olma, A. The biological consequences of replacing D-Ala in Biphalin with amphiphilic  $\alpha$ -alkylserines. *Chem. Biol. Drug Des.* **2014**, *84*, 199–205.
- (9) Fraczak, O.; Lasota, A.; Kosson, P.; Leśniak, A.; Muchowska, A.; Lipkowski, A. L.; Olma, A. Biphalin analogs containing  $\beta^3$ -homomino acids at the 4,4-positions: Synthesis and opioid activity profiles. *Peptides* **2015**, *66*, 13–18.
- (10) Hsieh, J.-Y.; Chiang, T.-Y.; Chen, J.-L.; Chen, Y.-W.; Lin, H.-C.; Hwang, C.-C. A molecular dynamics study on opioid activities of biphalin molecule. *J. Mol. Model.* **2011**, *17*, 2455–2464.
- (11) Mollica, A.; Davis, P.; Ma, S.-W.; Porreca, F.; Lai, J.; Hruby, V. J. Synthesis and biological activity of the first cyclic biphalin analogues. *Bioorg. Med. Chem. Lett.* **2006**, *16*, 367–372.
- (12) Mollica, A.; Carotenuto, A.; Novellino, E.; Limatola, A.; Costante, R.; Pinnen, F.; Stefanucci, A.; Pieretti, S.; Borsodi, A.

Samavati, R.; Zador, F.; Benyhe, S.; Davis, P.; Porreca, F.; Hruby, V. J. Novel cyclic biphalin analogue with improved antinociceptive properties. *ACS Med. Chem. Lett.* **2014**, *5*, 1032–1036.

(13) Smeenk, L. E. J.; Dailly, N.; Hiemstra, H.; van Maarseveen, J. H.; Timmerman, P. Synthesis of water-soluble scaffolds for peptide cyclization, labelling, and ligation. *Org. Lett.* **2012**, *14*, 1194–1197.

(14) Stefanucci, A.; Novellino, E.; Mirzaie, S.; Macedonio, G.; Pieretti, S.; Minosi, P.; Szűcs, E.; Erdei, A. I.; Zádor, F.; Benyhe, S.; Mollica, A. Opioid receptor activity and analgesic potency of DPDPE peptide analogues containing a xylene bridge. *ACS Med. Chem. Lett.* **2017**, *8*, 449–454.

(15) Mollica, A.; Pinnen, F.; Costante, R.; Locatelli, M.; Stefanucci, A.; Pieretti, S.; Davis, P.; Lai, J.; Rankin, D.; Porreca, F.; Hruby, V. J. Biological active analogues of the opioid peptide Biphalin: Mixed  $\alpha/\beta^3$ -peptides. *J. Med. Chem.* **2013**, *56*, 3419–3423.

(16) Smith, M. E. B.; Schumacher, F. F.; Ryan, C. P.; Tedaldi, L. M.; Papaioannou, D.; Waksman, G.; Caddick, S.; Baker, J. R. Protein modification, bioconjugation, and disulfide bridging using bromomaleimides. *J. Am. Chem. Soc.* **2010**, *132*, 1960–1965.

(17) Kowalczyk, R.; Harris, P. W. R.; Brimble, M. A.; Callon, K. E.; Watson, M.; Cornish, J. Synthesis and evaluation of disulphide bond mimetics of amylin-(1–8) as agents to treat osteoporosis. *Bioorg. Med. Chem.* **2012**, *20*, 2661–2668.

(18) Grieco, P.; Giusti, L.; Carotenuto, A.; Campiglia, P.; Calderone, V.; Lama, T.; Gomez-Monterrey, I.; Tartaro, G.; Mazzoni, M. R.; Novellino, E. Morphiceptin analogues containing a dipeptide mimetic structure: an investigation on the bioactive topology at the  $\mu$ -receptor. *J. Med. Chem.* **2005**, *48*, 3153–3163.

(19) Wüthrich, K. *NMR of Proteins and Nucleic Acids*; John Wiley & Sons: New York, 1986.

(20) Yamazaki, T.; Ro, S.; Goodman, M.; Chung, N. N.; Schiller, P. W. A topochemical approach to explain morphiceptin bioactivity. *J. Med. Chem.* **1993**, *36*, 708–719.

(21) Yamazaki, T.; Ro, S.; Goodman, M.; Chung, N. N.; Schiller, P. W.; Shenderovich, M. D.; Liao, S.; Qian, X.; Hruby, V. J. A three-dimensional model of the  $\delta$ -opioid pharmacophore: comparative molecular modeling of peptide and nonpeptide ligands. *Biopolymers* **2000**, *53*, 565–580.